# Effects of Ge substitution in GeTe by Ag or Sb on the Seebeck coefficient and carrier concentration derived from ^{125}Te NMR

E. M. Levin

Phys. Rev. B **93**, 045209 — Published 22 January 2016

DOI: 10.1103/PhysRevB.93.045209

12-22 -2015

# Effects of Ge substitution in GeTe by Ag or Sb on the Seebeck coefficient and carrier concentration derived from $^{125}$Te NMR

E. M. Levin

*Division of Materials Sciences and Engineering, U.S. Department of Energy Ames Laboratory, Ames, Iowa 50011, USA*
*Department of Physics and Astronomy, Iowa State University, Ames Iowa 50011, USA*

Submitted to *Physical Review B, Rapid Communications*

## Abstract

GeTe, a self-dopant *p*-type semiconductor, where the high free hole concentration is determined by Ge vacancies, is a well-known base for high-efficiency $Ag_xSb_xGe_{50-2x}Te_{50}$ (TAGS series) thermoelectric materials. Here it is shown that the replacement of Ge by Ag in GeTe ($Ag_xGe_{50-x}Te_{50}$ system) significantly decreases the Seebeck coefficient, while the replacement by Sb ($Sb_xGe_{50-x}Te_{50}$) increases it. These effects can be attributed to a change in carrier concentration and consistent with $^{125}$Te NMR spin-lattice relaxation measurements and NMR signal position, which is mostly dependent on the Knight shift. Opposite changes of carrier concentration in $Ag_xGe_{50-x}Te_{50}$ and $Sb_xGe_{50-x}Te_{50}$ can be explained by different valence electron configurations of Ag and Sb compared to that of Ge, which results in a different local electron imbalance and/or in a change of Ge vacancy formation energy and affects the total carrier concentration. Comparison of our data for GeTe, $Ag_2Ge_{48}Te_{50}$, and $Sb_2Ge_{48}Te_{50}$ with those for $Ag_2Sb_2Ge_{46}Te_{50}$ shows that the effects from Ag and Sb compensate for each other and supports the formation of [Ag+Sb] atomic pairs suggested earlier based on theoretical calculations.

**PACS:** 72.20.Pa; 76.60.-k; 76.60.Es

**Keywords:** GeTe alloyed with Ag or Sb; $^{125}$Te NMR spin-lattice relaxation; carrier concentration; Seebeck coefficient; electrical resistivity; power factor.

E-mail: levin@iastate.edu

Thermoelectric materials convert thermal energy to electricity via the Seebeck effect, a very interesting fundamental phenomenon observed in electrically conductive solids [1]. One well-known group of high-efficiency thermoelectric materials is based on the GeTe, where Ge is replaced by Ag and Sb forming $Ag_xSb_xGe_{50-2x}Te_{50}$ (Tellurium-Antimony-Germanium-Silver, TAGS) materials [2]. These materials show *p*-type (hole) conductivity and continue to attract great attention [3-5], while the origin of their high efficiency has never been explained. GeTe is *p*-type narrow-band semiconductor [6] with a high hole concentration, $8\times10^{20}$ $cm^{-3}$, generated by ~$4\times10^{20}$ $cm^{-3}$ Ge vacancies (each Ge vacancy generates two holes) [7,8], and exhibits gradual transformation of low-temperature rhombohedral to high-temperature cubic structure [8,9], which makes this compound very complex solid state system.

The Seebeck coefficient (or thermopower), *S*, and electrical resistivity, $\rho$, is used to estimate the power factor, $PF = S^2 / \rho$, which is a part of the thermoelectric figure of merit. Both the Seebeck coefficient and electrical resistivity are very sensitive to mobile charge carrier concentration, which can be controlled via chemical substitution. The goal of this work is to elucidate the effects of local electron imbalance on the Seebeck coefficient, electrical resistivity, power factor, and carrier concentration obtained from $^{125}$Te NMR, in GeTe-based materials where Ge is partially replaced by Ag ($Ag_xGe_{50-x}Te_{50}$ alloys) or Sb ($Sb_xGe_{50-x}Te_{50}$), and to compare the results to those in $Ag_2Sb_2Ge_{46}Te_{50}$.

Individual ingots of all alloys with a diameter of 10 mm and a length of ~40 mm were synthesized by the direct melting of the components in fused quartz ampoules at 1323 K. X-ray diffraction (XRD) patterns were obtained using a Rigaku Ultima U4 diffractometer at 300 K. Homogeneity and composition of all alloys was checked by scanning electron microscopy (SEM) and energy dispersive spectroscopy (EDS). $^{125}$Te nuclear magnetic resonance (NMR)

experiments were performed at 126 MHz using a Bruker 400WB plus spectrometer with TopSpin software in a magnetic field of 9.4 T without sample spinning (static regime). $^{125}$Te NMR chemical shifts were referenced to $Te(OH)_6$ in solution and chemical shifts relative to $(CH_3)_2Te$ in benzene were larger by +712 ppm [10]. $^{125}$Te NMR spin-lattice relaxation measurements were used to obtain the spin-lattice relaxation time, $T_1$, and free (mobile) charge carrier concentration, *p,* using GeTe as a reference material [8,10]. Measurements of the Seebeck coefficient and electrical resistivity were conducted simultaneously on the same sample using an LSR-3 measuring system (Linseis, Inc.) in a helium environment. Uncertainties in $T_1$ and $p$ measurements are 2% and 10%, respectively, while uncertainties in the Seebeck coefficient and electrical resistivity measurements are less than 5% and 3%, respectively. More details about sample preparation, XRD, $^{125}$Te NMR, Seebeck coefficient, electrical resistivity, SEM, and EDS measurements can be found in Refs. 5,8,10.

XRD shows that the replacement of Ge by Ag or Sb in GeTe can be represented by idealized solid solution compositions of $Ag_xGe_{50-x}Te_{50}$ or $Sb_xGe_{50-x}Te_{50}$ with an average composition close to the nominal. XRD shows the presence of a small amount of Ge inclusions in Sb-containing samples, but not in Ag-containing samples. SEM and EDS confirm the presence of small amounts of Ge (<2 at.%) inclusions in Sb-containing samples, similar to that observed in GeTe [8], and to a smaller extent in Ag-containing samples. In addition, EDS shows that the concentration of Ag and particularly Sb in these materials slightly varies along the sample reflecting their inhomogeneity.

Figure 1 presents temperature dependencies of the Seebeck coefficient of $Ag_xGe_{50-x}Te_{50}$ and $Sb_xGe_{50-x}Te_{50}$ alloys with $x$ = 2 and 4. No hysteresis in the Seebeck coefficient and electrical resistivity (both have been measured but are not shown here) during temperature cycling was

observed. Figure 2 demonstrates trends in $S$ and $\rho$ vs. Ag or Sb content in $Ag_xGe_{50-x}Te_{50}$ and $Sb_xGe_{50-x}Te_{50}$ alloys at 300 K and 750 K (see also Table 1). It is interesting that at 750 K, the Seebeck coefficient of $Ag_2Sb_2Ge_{46}Te_{50}$ containing 4 at.% of [Ag+Sb] shows the value close to that of GeTe, but higher than that of $Ag_4Ge_{46}Te_{50}$, and lower than that of $Sb_4Ge_{46}Te_{50}$ (Table 1). Within the Mott-Boltzmann formalism for systems with energy-independent charge carrier scattering, the Seebeck coefficient depends on the carrier concentration, $n$, of electrons or holes as $S \sim 1/n^{2/3}$ (e.g., see Ref. 1). The carrier concentration in semiconductors typically is deduced from Hall effect measurements. However, the Hall effect in multicomponent materials can be misleading due to the possible presence of separate phases particularly with different types of conductivity. For example, the Hall effect in *p*-type $AgSbTe_2$ shows *n*-type, which was attributed to the small amount of *n*-type $Ag_2Te$, while the Seebeck effect shows *p*-type, reflecting the major phase [11]. Potentially more reliable values of the carrier concentration and its distribution can be obtained from $^{125}$Te NMR spin-lattice relaxation measurements [10]. The Hall effect shows integral signal from all phases or local areas with non-uniform carrier concentration in a material, while $^{125}$Te NMR shows differential signals from each phase or local areas. This enables to better understand the Seebeck effect, which similar to the Hall effect shows integral signal from all phases or local areas. Note that in complex tellurides, local variation in chemical composition (while this cannot be detected by XRD) results in variation of the Seebeck coefficient, which can be attributed to the variation in carrier concentration and similar to the Hall effect can be misleading (see discussion below).

Figure 3 shows $^{125}$Te NMR spectra for GeTe (which confirm the position and shape of NMR signal for this compound reported in Refs. 8,10), and several $Ag_xGe_{50-x}Te_{50}$ and $Sb_xGe_{50-x}Te_{50}$ samples. Replacement of Ge by Ag shifts the signal from +160 ppm for GeTe to more

positive values while replacement of Ge by Sb shifts the signal to more negative values (Table 1). The $^{125}$Te NMR signal for $Ag_2Sb_2Ge_{46}Te_{50}$, similar to that reported in Ref. 12, is observed at +320 ppm, which is an intermediate value between those observed if only Ag or Sb atoms are present in the crystal lattice. Note that if Ag and Sb in the $Ag_2Sb_2Ge_{46}Te_{50}$ lattice are located far from each other, full width at half maximum (*FWHM*) of the $^{125}$Te NMR signal, estimated for $Ag_2Sb_{48}Te_{50}$ and $Sb_2Ge_{48}Te_{50}$ (see Fig. 3), is expected to be large, ~1200 ppm. In reality, the $^{125}$Te NMR signal for $Ag_2Sb_2Ge_{46}Te_{50}$ shows a much smaller *FWHM* = 510 ppm (Table 1).

Comparison of our $^{125}$Te NMR and Seebeck coefficient data for GeTe, $Ag_2Ge_{48}Te_{50}$, and $Sb_2Ge_{48}Te_{50}$ with those for $Ag_2Sb_2Ge_{46}Te_{50}$ shows that effects from Ag and Sb nearly compensate for each other. This can be explained (i) by the opposite effect (compensation) from Ag and Sb or (ii) by formation of [Ag+Sb] atomic pairs. Note that the Seebeck coefficient of $Ag_xSb_xGe_{50-2x}Te_{50}$ with $x \approx 6.5$ is very large compared to that of GeTe, +83 $\mu VK^{-1}$ and +193 $\mu VK^{-1}$ at 300 K and 750 K, respectively (similar large values were reported in Refs. 3,4), which means that there is no compensation from Ag and Sb here and is in favor of the existence of [Ag+Sb] pairs. Such pairs and a gradual transformation of the crystal structure from rhombohedral to cubic [8,9], can be responsible for the high efficiency of TAGS materials. Possible formation of [Ag+Sb] pairs in GeTe was theoretically studied by Hoang *et al*. [13] as well as in PbTe by Hazama *et al*. [14]; our $^{125}$Te NMR data support these theoretical calculations.

Spin-lattice relaxation in $Ag_2Ge_{48}Te_{50}$ can be fitted mostly by one component, $T_1$ = 2.0 ms, as well as in $Ag_4Ge_{46}Te_{50}$, $T_1$ = 1.6 ms, meaning that these alloys are mostly electronically and chemically homogeneous. In contrast, spin-lattice relaxation in $Sb_2Ge_{48}Te_{50}$ can be fitted by two components, $T_{1,A}$ = 3.2 ms and $T_{1,B}$ = 19.0 ms with fractions $f_A$ = 0.68 and $f_B$ = 0.32, (see details for fitting in Refs. 9,13). A similar situation is observed for $Sb_4Ge_{46}Te_{50}$ with $T_{1,A}$ = 3.0 ms and

$T_{1,B}$ = 30 ms with fractions $f_A$ = 0.39 and $f_B$ = 0.61, meaning that these alloys are electronically inhomogeneous.

Non-uniform carrier concentration in tellurides was suggested for PbTe-based materials based on microscale Seebeck scanning [15,16]. XRD, SEM, and EDS show chemically homogeneous materials, but Seebeck scanning demonstrates significant change its magnitude and even the presence of areas with *n*- or *p*-type conductivity [15]. This was explained by possible change in carrier concentration due to slight composition deviation [15,16], which for PbTe-based materials was also observed by $^{125}$Te NMR [10,17]. Similar inhomogeneity for GeTe-based materials shown here demonstrates that the change in carrier concentration due to variation of local composition is typical for multicomponent tellurides.

The Seebeck coefficient of $Sb_2Ge_{48}Te_{50}$ is +53 μV K$^{-1}$, which is larger than that of GeTe, +34 μV K$^{-1}$ (Table 1). This difference shows that despite the fraction with lower carrier concentration in $Sb_2Ge_{48}Te_{50}$ is small, $f_B$ = 032, possible contribution to the Seebeck coefficient from this fraction cannot be ignored and should be used to explain an increase of the Seebeck coefficient. It can be explained that existence of areas with lower carrier concentration (and larger Seebeck coefficient), which form series connection with areas of higher carrier concentration (and lower Seebeck coefficient) along the temperature gradient, will result in larger bulk (integral) Seebeck coefficient. Certainly, the bulk value depends on the spatial distribution of these areas. In $Sb_4Ge_{46}Te_{50}$, the fraction with lower concentration is larger, $f_B$ = 0.61, and the bulk Seebeck coefficient is larger, +86 μV K$^{-1}$ (Table 1), i.e. the contribution from the fraction with lower carrier concentration increases.

With Maxwell-Boltzmann statistics (used for semiconductors), the carrier concentration and spin-lattice relaxation time are related as $1/T_1 \sim n$, while with Fermi-Dirac statistics (used

for metals) $1/T_1 \sim n^{2/3}$ [18,19]. At the given temperature $n = n_r(T_{1,r}/T_1)$ (Maxwell-Boltzmann statistics), and using GeTe as a reference material with $T_{1,r} = 5.3 \pm 0.2$ ms from $^{125}$Te NMR [8,10] and $p = 8\times10^{20}$ cm$^{-3}$ from the Hall effect [5,7,20], we can calculate the corresponding hole concentration via the equation $p = 4.24\times10^{21}/T_1$ cm$^{-3}$ ($T_1$ in ms, $p$ in cm$^{-3}$) [10] in $Ag_2Ge_{48}Te_{50}$ and $Ag_4Ge_{46}Te_{50}$ [Fig. 4(a) and Table 1]. The hole carrier concentrations estimated for $Sb_2Ge_{48}Te_{50}$ and $Sb_4Ge_{46}Te_{50}$ for a short and long $T_1$ are in general lower than that in Ag containing samples (Table 1). The carrier concentrations in $Ag_xGe_{50-x}Te_{50}$ and $Sb_xGe_{50-x}Te_{50}$ calculated from $T_1$ using Fermi-Dirac statistics is different [see comparison on Fig. 4(a)], but the trends observed for these materials is the same: Ag increases the carrier concentration, while Sb decreases it. Hall effect measurements at 300 K confirm that this trend, showing that the carrier concentration in $Ag_xGe_{50-x}Te_{50}$ is higher, $17\times10^{20}$ cm$^{-3}$ ($x$=2) and $30\times10^{20}$ cm$^{-3}$ ($x$=4), compared to that in GeTe, and lower in $Sb_xGe_{50-x}Te_{50}$, $4\times10^{20}$ cm$^{-3}$ ($x$=2) and $2.3\times10^{20}$ cm$^{-3}$ ($x$=4), which are between those obtained from $^{125}$Te NMR long and short $T_1$ (Table 1). The values of the carrier concentrations in $Sb_xGe_{50-x}Te_{50}$ obtained from the Hall effect are between those obtained from NMR. This shows that the high Hall voltage from the low-carrier concentration dominates the low Hall voltage from the high-carrier concentration, but the total Hall voltage is reduced.

It is possible to estimate changes in carrier concentration if Ge in GeTe is replaced by Ag or Sb. There are $1.85\times10^{22}$ cm$^{-3}$ Ge atoms in ideal GeTe. If one Ag atom replaces one Ge out of 50 in $Ge_{50}Te_{50}$ and results in one hole, the additional carrier concentration should be $3.7\times10^{20}$ cm$^{-3}$; two Ag atoms result in $7.4\times10^{20}$ cm$^{-3}$. The total concentration (background in GeTe, $8\times10^{20}$ cm$^{-3}$, plus contribution due to two Ag) will be $15.4\times10^{20}$ cm$^{-3}$. This value is close to that obtained from the Hall effect and $^{125}$Te NMR spin-lattice relaxation measurements. Similarly, if one Sb atom replaces Ge and reduces the carrier concentration by one hole, the reduction due to two Sb

atoms should be $7.4\times10^{20}$ $cm^{-3}$, and the total carrier concentration should be reduced to $0.6\times10^{20}$ $cm^{-3}$. This value is smaller compared to that obtained by NMR and Hall effect measurements and shows that Sb may have lower doping efficiency compared to Ag. The differences observed also can be attributed to change in concentration of Ge vacancies: Ag can reduce the energy of formation of Ge vacancy, while Sb can increase it. Let's suggest that Ag and Sb affect only the concentration of Ge vacancies; note that there are ~$4\times10^{20}$ $cm^{-3}$ (or ~2%) naturally occurring Ge vacancies in GeTe. If Ag results in more Ge vacancies, ~$10\times10^{20}$ $cm^{-3}$ (or ~5%) Ge vacancies are needed to explain an increase of the carrier concentration in $Ag_2Ge_{48}Te_{50}$. Similarly, if Sb results in less Ge vacancies, ~$1\times10^{20}$ $cm^{-3}$ (~0.5%) Ge vacancies are needed to explain a decrease of the carrier concentration in $Sb_2Ge_{48}Te_{50}$. All scenarios shown above seem to be realistic.

Selbach *et al*. [18] also showed similar dependencies containing the carrier effective mass, $m^*$, $1/T_1 \sim (m^*)^{3/2} n$ with Maxwell-Boltzmann statistics or $1/T_1 \sim (m^*)^2 n^{2/3}$ with Fermi-Dirac statistics, which demonstrate that $m^*$ can also affect the relation between $T_1$ and $n$, and needs to be studied in more detail. However, the large shifts in the $^{125}$Te NMR spectra correlate well with the changes in $T_1$, showing that a major effect on $T_1$ in $Ag_xGe_{50-x}Te_{50}$ and $Sb_xGe_{50-x}Te_{50}$ arises from the carrier concentration. Note also that the $T_1$ values across the $^{125}$Te NMR spectrum in GeTe change insignificantly, showing that the large broadening, 460 ppm, cannot be attributed only to the distribution of Knight shifts.

The position of the NMR signal in electrically conductive materials is typically expressed via the total shift, $\delta_{total}$, relative to the reference material: $\delta_{total} = \delta_{chem} + K$, where $\delta_{chem}$ is the chemical shift due to the environment around Te atoms, and $K$ is the Knight shift due to the effect of the hyperfine interaction between nuclei and free (mobile) charge carriers and strongly depends on the carrier concentration [18,19]. The Knight shift, $K$, and spin-lattice relaxation

time, $T_1$, are related via the Korringa relation $K^2T_1T = const$, where $T$ is the absolute temperature [19], and at constant temperature the Korringa relation can be shown as $K^2T_1$ = constant [21]. Note that GeTe, $Ag_xGe_{50-x}Te_{50}$, and $Sb_xGe_{50-x}Te_{50}$ show diamagnetic properties in a temperature range of 1.8-300 K and magnetic fields of 0-50 kOe (data not shown), which allows us to conclude that the Korringa mechanism of relaxation is the dominant one. Measurements of $T_1$ enable us to estimate the contributions to the resonance positions from $K$ and $\delta_{chem}$ in $Ag_xGe_{50-x}Te_{50}$ and $Sb_xGe_{50-x}Te_{50}$. At the same temperature, $K = K_r(T_{1,r}/T_1)^{1/2}$ where $K_r$ and $T_{1,r}$ are the Knight shift and spin-lattice relaxation time of a reference material, GeTe. The Knight shift of GeTe can be determined as $K = \delta_{total} - \delta_{chem}$, where $\delta_{total}$ = +160 ppm [8], $\delta_{chem}$ = -890 ppm [22] so $K$ = +1050 ppm. The Knight shift estimated from $T_1$ for $Ag_2Ge_{48}Te_{50}$ is about +1700 ppm, and for $Sb_2Ge_{48}Te_{50}$ using long $T_1$ components is +600 ppm, i.e., they are larger and smaller than that of GeTe, respectively, which explains the position of $^{125}$Te NMR signals (Fig. 3).

In general, Ag in GeTe serves as a donor, while Sb as an acceptor. However, the effect of chemical substitution via alloying in GeTe is quite different compared to that in semiconductors like Si, where donors (P) create mobile electrons (*n*-type conductivity) directly in the conduction band, while acceptors (B) create mobile holes (*p*-type conductivity) in the valence band. Although GeTe is a semiconductor, the temperature dependence of its electrical resistivity is typical for that of metals up to 800 K [8], which can be explained by a high carrier concentration generated by Ge vacancies [7]. $Ag_xGe_{50-x}Te_{50}$ and $Sb_xGe_{50-x}Te_{50}$ also exhibit metallic conductivity (not show here), which demonstrates that the analysis of these materials can be conducted upon the assumption of a degenerate electronic (metallic) state in these materials [23].

Opposite changes of carrier concentration in $Ag_xGe_{50-x}Te_{50}$ and $Sb_xGe_{50-x}Te_{50}$ can be explained by different valence electron configurations of Ag and Sb compared to that of Ge,

which results in a different local electron imbalance and/or in a change of Ge vacancy formation energy, and affects the total carrier concentration. DFT calculations for pure GeTe by Edwards *et al*. [24] show that (i) Ge vacancy has very low formation energy, and (ii) the presence of Ge vacancies in large numbers leads to a large concentration of holes in the valence band. In principle, Ag can also decrease this energy, while Sb can increase it and this may result in a higher or lower concentration of Ge vacancies and change the total carrier concentration.

A total hole concentration, $p_{total}$, in GeTe-based materials containing Ag or Sb may consist of contributions from: (i) Ge vacancies (two holes per vacancy) producing the base hole concentration, $p_{base}$, and dependent mostly on the Ge/Te ratio, and contributions (ii) due to Ag at a Ge site producing an additional hole and/or more Ge vacancies and resulting in $p_{total} > p_{base}$, and (iii) due to Sb at a Ge site producing one electron and due to its compensation in *p*-type GeTe matrix and or less Ge vacancies resulting in $p_{total} < p_{base}$. In $Ag_2Sb_2Ge_{46}Te_{50}$ the numbers of Ag and Sb atoms are nearly equal and $p_{total} \approx p_{\text{base}}$, which follows from both the value of the Seebeck coefficient and the $^{125}$Te NMR data. Nevertheless, the replacement of Ge in GeTe by Ag or Sb can significantly increase or decrease the free carrier concentration respectively [Fig. 4(a)].

Our data for the electronically homogeneous $Ag_xGe_{50-x}Te_{50}$ system can be explained, in general, using the $S \sim 1/n^{2/3}$ dependence. Note that the values of the Seebeck coefficient calculated using the carrier concentration extracted from $T_1$ NMR analysis with Maxwell Boltzmann statistic fit better than those obtained with Fermi-Dirac statistics. Data for the electronically inhomogeneous $Sb_xGe_{50-x}Te_{50}$ system show that the observed larger Seebeck coefficient (Fig. 1) should be attributed mostly to the charge carriers of lower concentration

(associated with longer $T_1$); some effect from the carriers with higher carrier concentration (associated with shorter $T_1$) cannot be excluded.

The carrier concentration in both $Ag_xGe_{50-x}Te_{50}$ and $Sb_xGe_{50-x}Te_{50}$ changes nonlinearly showing a limitation in the solubility of Ag and Sb. The carrier concentration in $Ag_2Sb_2Ge_{46}Te_{50}$ calculated using $T_1 = 3.6$ ms,[12] is $12\times10^{20}$ cm$^{-3}$, just slightly larger when compared to that in GeTe [Fig. 4(a)]. Similarly, the values of the Seebeck coefficient and electrical resistivity [Figs. 2(a)(b)] are close to those in GeTe. Interplay between the Seebeck coefficient and electrical resistivity in $Ag_xGe_{50-x}Te_{50}$ and $Sb_xGe_{50-x}Te_{50}$ alloys significantly affects the power factor [Fig. 4(b)]. The largest value of $PF = 46$ μW cm$^{-1}$ K$^{-2}$ was found for $Sb_2Ge_{48}Te_{50}$, which is even higher than that of GeTe, 42 μW cm$^{-1}$ K$^{-2}$, reported in Ref. 8 and confirmed by Sun *et al*. [25], and is one of the highest values observed for high efficiency thermoelectric tellurides.

In summary, the replacement of Ge in a *p*-type self-doping GeTe semiconductor by Ag or Sb in $Ag_xGe_{50-x}Te_{50}$ or $Sb_xGe_{50-x}Te_{50}$ alloys form solid solutions with an insignificant amount of separate phases. Ag decreases the Seebeck coefficient while Sb increases it, which according to $^{125}$Te NMR spectra and spin-lattice relaxation time can be explained by the respective increase or decrease of the carrier concentration. Two approaches based on Maxwell-Boltzmann (for semiconductors) and Fermi-Dirac (for metals) statistics, which describe the relation between the carrier concentration and NMR spin-lattice relaxation time, were used to calculate the carrier concentration and showed similar trends. Comparison of our data for GeTe, $Ag_2Ge_{48}Te_{50}$, and $Sb_2Ge_{48}Te_{50}$ with those for $Ag_2Sb_2Ge_{46}Te_{50}$ shows that the effects from Ag and Sb compensate for each other and supports the formation of [Ag+Sb] atomic pairs suggested earlier based on theoretical calculations.

The author thanks the Materials Preparation Center at the Ames Laboratory U.S. Department of Energy (DOE) for sample synthesis, W.E. Straszheim and S.L. Bud'ko for help in experiments, and K. Schmidt-Rohr for interest in this research. This work was supported by the U.S. Department of Energy, Office of Basic Energy Sciences, Division of Materials Sciences and Engineering. The research was performed at the Ames Laboratory, which is operated for the U.S. Department of Energy by Iowa State University under Contract No DE-AC02-07CH11358.

[1] G. J. Snyder and E. S. Toberer. Nature Mater. **7**, 105 (2008).

[2] E. A. Skrabek and D.S. Trimmer. In *CRC Handbook of Thermoelectrics* (Ed. by D.M. Rowe) CRC Press LLC, 1995, chapter 22.

[3] S. H. Yang, T. J. Zhu, T. Sun, J. He, S. N. Zhang, and X. B. Zhao. Nanotechnology **19**, 245707 (2008).

[4] J. R. Salvador, J. Yang, X. Shi, H. Wang, and A. A. Wereszczak. J. Solid State Chem. **182**, 2088 (2009).

[5] E. M. Levin, S. L. Bud'ko, and K. Schmidt-Rohr. Adv. Funct. Mater. **22**, 2766 (2012).

[6] P. M. Nikolic, Brit. J. Appl. Phys. (J. Phys. D) **2**, 383 (1969).

[7] M. S. Lubell and R. Mazelsky. J. Electrochem. Soc. **110**, 520 (1963).

[8] E. M. Levin, M. F. Besser, and R. Hanus. J. Appl. Phys. **114**, 083713 (2013).

[9] T. Chattopadhyay, J.X. Boucherle, and H.G. von Schnering, J. Phys. C: Solid State Phys. **20**, 1431 (1987).

[10] E. M. Levin, J. P. Heremans, M. G. Kanatzidis, and K. Schmidt-Rohr. Phys. Rev. B **88**, 115211 (2013).

[11] R. Wolfe, J.H. Wernick, and.E. Haszko. J. Appl. Phys. **31**, 1959 (1960).

[12] E. M. Levin, R. Hanus, M. Hanson, W. E. Straszheim, and K. Schmidt-Rohr. Phys. Status Solidi A **210**, 2628 (2013).

[13] K. Hoang, S. D. Mahanti, and M. G. Kanatzidis. Phys. Rev. B **81**, 115106 (2010)

[14] H. Hazama, U. Mizutani, and R. Asahi. Phys. Rev. B **73**, 115108 (2006).

[15] N. Chen, F. Gascoin, G.J. Snyder, E. Muller, G. Karpinski, and C. Stiewe. J. Appl. Phys. Lett. **87**, 171903 (2005).

[16] A. Kosuga, K. Kurosaki, H. Muta, C. Stiewe, G. Karpinski, E. Muller, and S. Yamanaka. Mater. Trans. **47**, 1440 (2006).

[17] 16. E.M. Levin, B.A. Cook, K. Ahn, M.G. Kanatzidis, and K. Schmidt-Rohr. Phys. Rev. B **80**, 115211 (2009).

[18] H. Selbach, O. Kanert, and D. Wolf. Phys. Rev. B **19**, 4435 (1979).

[19] J. P. Yesinowski. Top Curr. Chem. **306**, 229 (2012).

[20] Y. Gelbstein, B. Daro, O. Ben-Yehuda, Y. Sadia, Z. Dashevsky, and M. P. Dariel. J. Electron. Mater. **39**, 2049 (2010).

[21] J. P. Yesinowski, A. P. Purdy, H. Wu, M. G. Spencer, J. Hunting, and F. J. DiSalvo. J. Am. Chem. Soc. **128**, 4952 (2006).

[22] B. Njegic, E. M. Levin, and K. Schmidt-Rohr. Solid State Nucl. Magn. Reson. **55-56**, 79 (2013).

[23] R. Shaltaf, X. Gonze, M. Cardona, R. K. Kremer, and G. Siegle. Phys. Rev. B 79, 075204 (2009).

[24] A.H. Edwards, A.C. Pineda, P.A. Schultz, M.G. Martin, A.P. Thompson, H.P. Hjamarson, C.J. Umrigar, Phys. Rev. B **73**, 045210 (2006).

[25] H. Sun, X. Lu, H. Chi, D. T. Morelli, and C. Uher. Phys. Chem. Chem. Phys. **16**, 15570 (2014).

Table 1. Composition, Seebeck coefficient, $S$, electrical resistivity, $\rho$, $^{125}$Te NMR peak position (i.e., the total shift, $\delta_{total}$), full width at half maximum (*FWHM*), spin-lattice relaxation time, $T_1$, and the carrier concentration, $p$, obtained from $T_1$ using Maxwell-Boltzmann statistics.

| Composition | $S$ ($\mu V\ K^{-1}$) | | $\rho$ ($\mu\Omega$ m) | | $\delta_{total}$ (ppm) 300 K | *FWHM* (ppm) 300 K | Spin-lattice relaxation time* and fraction 300 K | $p$ ($cm^{-3}$) 300 K |
|---|---|---|---|---|---|---|---|---|
| | 300 K | 750 K | 300 K | 750 K | | | | |
| GeTe | +34 | +163 | 1.4 | 6.4 | +160 | 440 | $T_1$=5.3 ms | $8\times10^{20}$ |
| $Ag_2Ge_{48}Te_{50}$ | +26 | +116 | 1.6 | 3.7 | +620 | 480 | $T_1$=2.0 ms | $20\times10^{20}$ |
| $Ag_4Ge_{48}Te_{50}$ | +25 | +94 | 2.2 | 3.6 | +730 | 530 | $T_1$=1.6 ms | $25\times10^{20}$ |
| $Sb_2Ge_{48}Te_{50}$ | +53 | +180 | 2.0 | 6.9 | -30 | 550 | $T_{1,A}$=3.2 ms, $f_A$=0.68<br>$T_{1,B}$=19.0 ms, $f_B$=0.32 | $14\times10^{20}$<br>$2\times10^{20}$ |
| $Sb_4Ge_{46}Te_{50}$ | +86 | +211 | 4.2 | 10.8 | -460 | 550 | $T_{1,A}$=3.0 ms, $f_A$=0.39<br>$T_{1,B}$=30.0 ms, $f_B$ =0.61 | $14\times10^{20}$<br>$1.4\times10^{20}$ |
| $Ag_2Sb_2Ge_{46}Te_{50}$ | +39 | +154 | 2.2 | 5.5 | +320 | 510 | $T_1$=3.6 ms | $12\times10^{20}$ |

* Can fit by one, $T_1$, or two components, $T_{1,A}$ and $T_{1,B}$, with fractions $f_A$ and $f_B$.

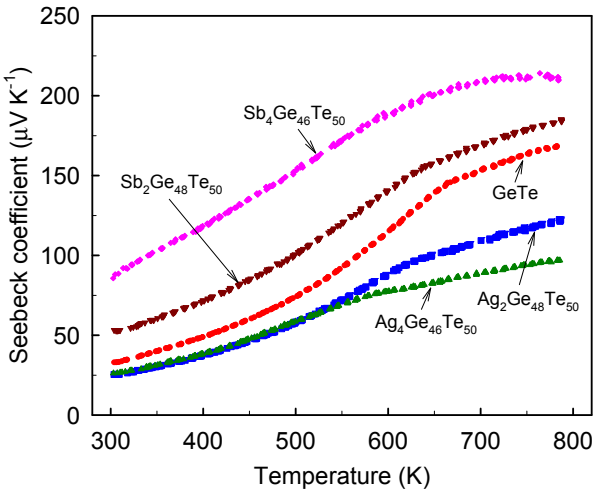


FIG. 1. Temperature dependences of the absolute Seebeck coefficient of $Ag_xGe_{50-x}Te_{50}$ and $Sb_xGe_{50-x}Te_{50}$ alloys. Data for GeTe shown for comparison.

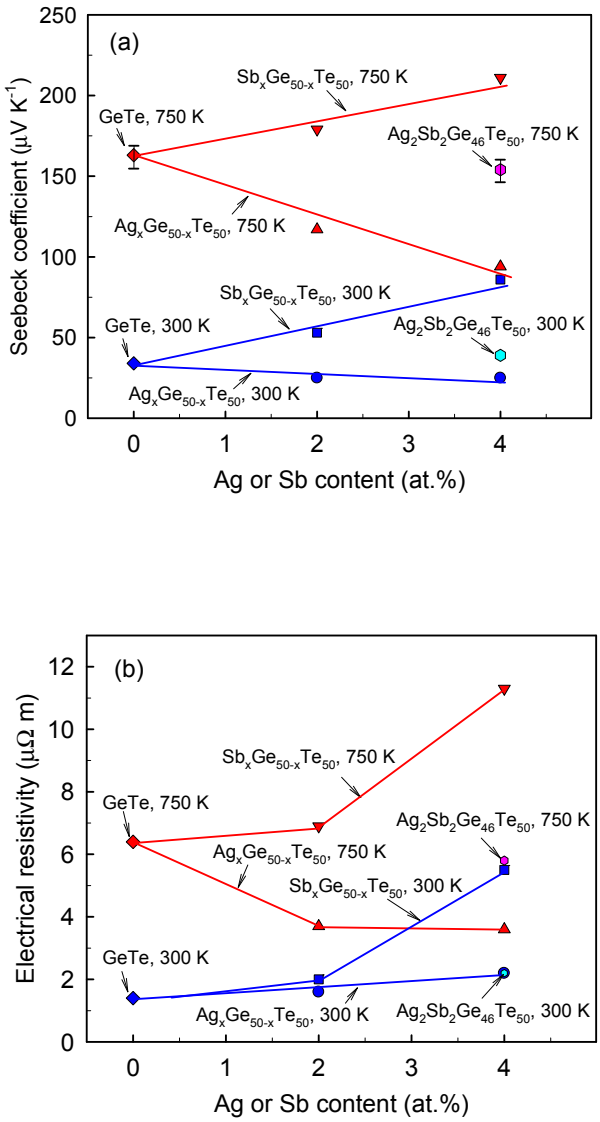


FIG. 2. Dependencies of the (a) Seebeck coefficient and (b) electrical resistivity of $Ag_xGe_{50-x}Te_{50}$ and $Sb_xGe_{50-x}Te_{50}$ at 300 K and 750 K vs. Ag or Sb content. Data for $Ag_2Sb_2Ge_{46}Te_{50}$ shown for comparison.

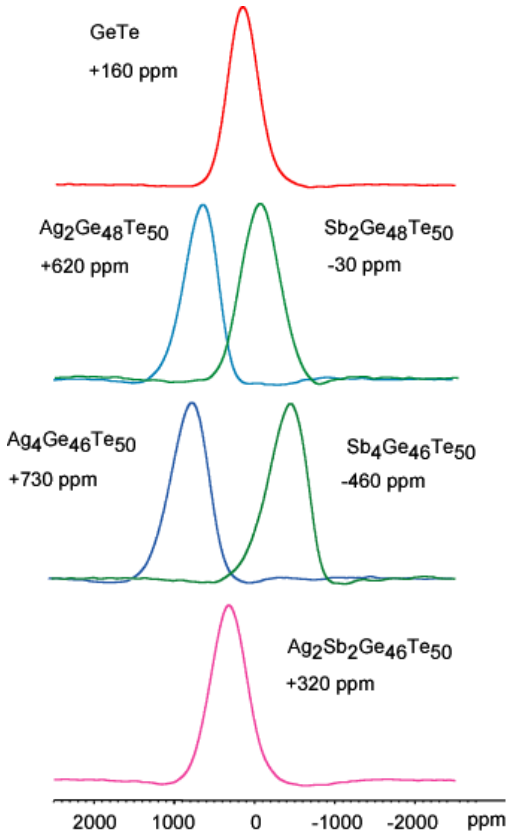


FIG. 3. $^{125}$Te NMR spectra (static regime) of *p*-type GeTe, $Ag_xSb_{50-x}Te_{50}$, $Sb_xSb_{50-x}Te_{50}$ and $Ag_2Sb_2Ge_{46}Te_{50}$ at 300 300 K obtained for 50-ms saturated recovery time.

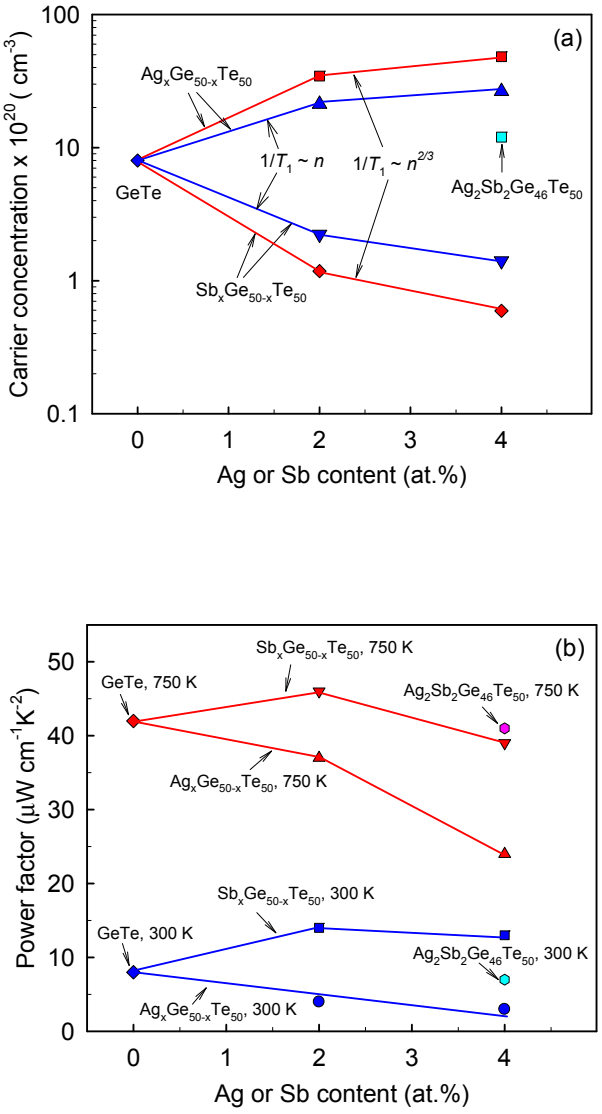


FIG. 4. (a) The carrier concentration obtained from $^{125}$Te NMR spin-lattice relaxation measurements at 300 K using $1/T_1 \sim n$ (with Maxwell-Boltzmann statistics) and $1/T_1 \sim n^{2/3}$ (with Fermi-Dirac statistics) relations, and (b) power factor of $Ag_xGe_{50-x}Te_{50}$ and $Sb_xGe_{50-x}Te_{50}$ vs. Ag or Sb content at 300 K and 750 K.